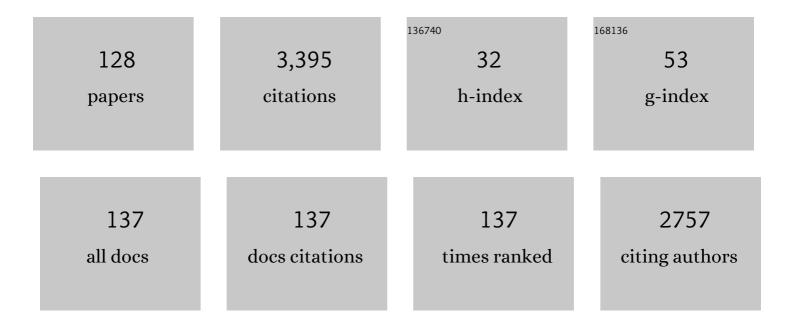
Aju P Pazhenkottil

List of Publications by Year in descending order

Source: https://exaly.com/author-pdf/6629032/publications.pdf Version: 2024-02-01



#	Article	IF	CITATIONS
1	Transluminal attenuation gradient derived from coronary CT angiography to predict ischemia in SPECT myocardial perfusion imaging: Effect of coronary cross-sectional area. Journal of Nuclear Cardiology, 2022, 29, 350-358.	1.4	1
2	Splenic switch-off as a novel marker for adenosine response in nitrogen-13 ammonia PET myocardial perfusion imaging: Cross-validation against CMR using a hybrid PET/MR device. Journal of Nuclear Cardiology, 2022, 29, 1205-1214.	1.4	12
3	Radiation dose reduction with deep-learning image reconstruction for coronary computed tomography angiography. European Radiology, 2022, 32, 2620-2628.	2.3	21
4	Prospective association between pro-inflammatory state on admission and posttraumatic stress following acute coronary syndrome. General Hospital Psychiatry, 2022, 74, 58-64.	1.2	2
5	Assessment of Artificial Intelligence in Echocardiography Diagnostics in Differentiating Takotsubo Syndrome From Myocardial Infarction. JAMA Cardiology, 2022, 7, 494.	3.0	18
6	Association Between Changes in Post-hospital Cardiac Symptoms and Changes in Acute Coronary Syndrome-Induced Symptoms of Post-traumatic Stress. Frontiers in Cardiovascular Medicine, 2022, 9, 852710.	1.1	1
7	Risk stratification using coronary artery calcium scoring based on low tube voltage computed tomography. International Journal of Cardiovascular Imaging, 2022, 38, 2227-2234.	0.2	1
8	Sleep disturbance after acute coronary syndrome: A longitudinal study over 12 months. PLoS ONE, 2022, 17, e0269545.	1.1	2
9	Psychosocial and clinical characteristics of a patient with Takotsubo syndrome and her healthy monozygotic twin: a case report. European Heart Journal - Case Reports, 2022, 6, .	0.3	1
10	Value of 12-lead electrocardiogram to predict myocardial scar on FDG PET in heart failure patients. Journal of Nuclear Cardiology, 2021, 28, 1364-1373.	1.4	12
11	Role of quantitative myocardial blood flow and 13N-ammonia washout for viability assessment in ischemic cardiomyopathy. Journal of Nuclear Cardiology, 2021, 28, 263-273.	1.4	13
12	Innervation imaging to guide ventricular arrhythmia ablation. Journal of Nuclear Cardiology, 2021, 28, 184-186.	1.4	0
13	Myocardial creep-induced misalignment artifacts in PET/MR myocardial perfusion imaging. European Journal of Nuclear Medicine and Molecular Imaging, 2021, 48, 406-413.	3.3	4
14	Quantification of perivascular inflammation does not provide incremental prognostic value over myocardial perfusion imaging and calcium scoring. European Journal of Nuclear Medicine and Molecular Imaging, 2021, 48, 1806-1812.	3.3	17
15	Prognostic Value of Quantitative Metrics From Positron Emission Tomography in Ischemic HeartÂFailure. JACC: Cardiovascular Imaging, 2021, 14, 454-464.	2.3	16
16	Coronary artery lumen volume index as a marker of flow-limiting atherosclerosis—validation against 13N-ammonia positron emission tomography. European Radiology, 2021, 31, 5116-5126.	2.3	1
17	Age- and sex-dependent changes of resting amygdalar activity in individuals free of clinical cardiovascular disease. Journal of Nuclear Cardiology, 2021, 28, 427-432.	1.4	4
18	Splenic switch-off as a predictor for coronary adenosine response: validation against 13N-ammonia during co-injection myocardial perfusion imaging on a hybrid PET/CMRÂscanner. Journal of Cardiovascular Magnetic Resonance, 2021, 23, 3.	1.6	12

#	Article	IF	CITATIONS
19	Insomnia Symptoms and Acute Coronary Syndrome-Induced Posttraumatic Stress Symptoms: A Comprehensive Analysis of Cross-sectional and Prospective Associations. Annals of Behavioral Medicine, 2021, 55, 1019-1030.	1.7	3
20	Potential Impact of Statins on Neuronal Stress Responses in Patients at Risk for Cardiovascular Disease. Journal of Personalized Medicine, 2021, 11, 261.	1.1	2
21	Course, Moderators, and Predictors of Acute Coronary Syndrome-Induced Post-traumatic Stress: A Secondary Analysis From the Myocardial Infarction-Stress Prevention Intervention Randomized Controlled Trial. Frontiers in Psychiatry, 2021, 12, 621284.	1.3	9
22	Prognostic value of regional myocardial flow reserve derived from 13N-ammonia positron emission tomography in patients with suspected coronary artery disease. European Journal of Nuclear Medicine and Molecular Imaging, 2021, 49, 311-320.	3.3	5
23	Longitudinal association between cognitive depressive symptoms and Dâ€dimer levels in patients following acute myocardial infarction. Clinical Cardiology, 2021, 44, 1316-1325.	0.7	4
24	Serum cortisol as a predictor for posttraumatic stress disorder symptoms in post-myocardial infarction patients. Journal of Affective Disorders, 2021, 292, 687-694.	2.0	7
25	Depressive symptoms in patients after primary and secondary prophylactic ICD implantation. Clinical Research in Cardiology, 2021, , 1.	1.5	0
26	Sex and age differences in the association of heart rate responses to adenosine and myocardial ischemia in patients undergoing myocardial perfusion imaging. Journal of Nuclear Cardiology, 2020, 27, 159-170.	1.4	11
27	New insights in the assessment of left ventricular dyssynchrony: Laying the foundations for phase analysis by cardiac SPECT. Journal of Nuclear Cardiology, 2020, 27, 2280-2282.	1.4	0
28	Ultra-low-dose computed tomography for attenuation correction of cadmium-zinc-telluride single photon emission computed tomography myocardial perfusion imaging. Journal of Nuclear Cardiology, 2020, 27, 228-237.	1.4	10
29	"Apical thinningâ€ŧ Relations between myocardial wall thickness and apical left ventricular tracer uptake as assessed with positron emission tomography myocardial perfusion imaging. Journal of Nuclear Cardiology, 2020, 27, 452-460.	1.4	9
30	Association between vertebral bone mineral density, myocardial perfusion, and long-term cardiovascular outcomes: A sex-specific analysis. Journal of Nuclear Cardiology, 2020, 27, 726-736.	1.4	7
31	Sex-dependent association between inflammation, neural stress responses, and impaired myocardial function. European Journal of Nuclear Medicine and Molecular Imaging, 2020, 47, 2010-2015.	3.3	19
32	Coronary artery volume index: a novel CCTA-derived predictor for cardiovascular events. International Journal of Cardiovascular Imaging, 2020, 36, 713-722.	0.7	6
33	Diagnostic criteria for left ventricular non-compaction in cardiac computed tomography. PLoS ONE, 2020, 15, e0235751.	1.1	7
34	Myocardial 18F-FDG Uptake Pattern for Cardiovascular Risk Stratification in Patients Undergoing Oncologic PET/CT. Journal of Clinical Medicine, 2020, 9, 2279.	1.0	14
35	Relationship between job burnout and somatic diseases: a network analysis. Scientific Reports, 2020, 10, 18438.	1.6	25
36	Potential of Radiation Dose Reduction by Optimizing Z-Axis Coverage in Coronary Computed Tomography Angiography on a Latest-Generation 256-Slice Scanner. Journal of Computer Assisted Tomography, 2020, 44, 289-294.	0.5	1

#	Article	IF	CITATIONS
37	Microvascular dysfunction and sympathetic hyperactivity in women with supra-normal left ventricular ejection fraction (snLVEF). European Journal of Nuclear Medicine and Molecular Imaging, 2020, 47, 3094-3106.	3.3	25
38	Angiosarcoma Involving the Heart. New England Journal of Medicine, 2020, 382, 855-855.	13.9	4
39	Validation of deep-learning image reconstruction for coronary computed tomography angiography: Impact on noise, image quality and diagnostic accuracy. Journal of Cardiovascular Computed Tomography, 2020, 14, 444-451.	0.7	105
40	Expert recommendation from the Swiss Amyloidosis Network (SAN) for systemic AL-amyloidosis. Swiss Medical Weekly, 2020, 150, w20364.	0.8	10
41	Impact of Adaptive Statistical Iterative Reconstruction-V on Coronary Artery Calcium Scores Obtained From Low-Tube-Voltage Computed Tomography – A Patient Study. Academic Radiology, 2020, , .	1.3	3
42	High efficiency gamma camera enables ultra-low fixed dose stress/rest myocardial perfusion imaging. European Heart Journal Cardiovascular Imaging, 2019, 20, 218-224.	0.5	12
43	No differences in rest myocardial blood flow in stunned and hibernating myocardium: insights into the pathophysiology of ischemic cardiomyopathy. European Journal of Nuclear Medicine and Molecular Imaging, 2019, 46, 2322-2328.	3.3	9
44	Enhanced radiation exposure associated with anterior-posterior x-ray tube position in young women undergoing cardiac computed tomography. American Heart Journal, 2019, 215, 91-94.	1.2	4
45	Heart rate reserve is a long-term risk predictor in women undergoing myocardial perfusion imaging. European Journal of Nuclear Medicine and Molecular Imaging, 2019, 46, 2032-2041.	3.3	12
46	Sex Differences in the Association between Inflammation and Ischemic Heart Disease. Thrombosis and Haemostasis, 2019, 119, 1471-1480.	1.8	22
47	Metabolic Activity in Central Neural Structures of Patients With Myocardial Injury. Journal of the American Heart Association, 2019, 8, e013070.	1.6	4
48	Quantification of intrathoracic fat adds prognostic value in women undergoing myocardial perfusion imaging. International Journal of Cardiology, 2019, 292, 258-264.	0.8	9
49	Association between resting amygdalar activity and abnormal cardiac function in women and men: a retrospective cohort study. European Heart Journal Cardiovascular Imaging, 2019, 20, 625-632.	0.5	24
50	Heart rate reserve during pharmacological stress is a significant negative predictor of impaired coronary flow reserve in women. European Journal of Nuclear Medicine and Molecular Imaging, 2019, 46, 1257-1267.	3.3	18
51	Association between beta-adrenoceptor antagonist-induced sympathicolysis and severity of coronary artery disease as assessed by coronary computed tomography angiography (CCTA). International Journal of Cardiovascular Imaging, 2019, 35, 927-936.	0.7	1
52	Cardiac hybrid imaging combining 3D-strain echocardiography with coronary computed tomography angiography. European Heart Journal, 2019, 40, 395-396.	1.0	4
53	Corrected coronary opacification decrease from coronary computed tomography angiography: Validation with quantitative 13N-ammonia positron emission tomography. Journal of Nuclear Cardiology, 2019, 26, 561-568.	1.4	13
54	Cardiac resynchronization therapy in chronic heart failure: Effect on right ventricular function. Journal of Nuclear Cardiology, 2019, 26, 133-135.	1.4	3

#	Article	IF	CITATIONS
55	Gated SPECT myocardial perfusion imaging with cadmium-zinc-telluride detectors allows real-time assessment of dobutamine-stress-induced wall motion abnormalities. Journal of Nuclear Cardiology, 2019, 26, 1734-1742.	1.4	3
56	Sports Behavior in Middle-Aged Individuals with Anomalous Coronary Artery from the Opposite Sinus of Valsalva. Cardiology, 2018, 139, 222-230.	0.6	7
57	Impact of cardiac hybrid imaging-guided patient management on clinical long-term outcome. International Journal of Cardiology, 2018, 261, 218-222.	0.8	12
58	Ultra-low-dose coronary artery calcium scoring using novel scoring thresholds for low tube voltage protocols—a pilot study. European Heart Journal Cardiovascular Imaging, 2018, 19, 1362-1371.	0.5	34
59	Non-invasive screening for coronary artery disease in asymptomatic diabetic patients: a systematic review and meta-analysis of randomised controlled trials. European Heart Journal Cardiovascular Imaging, 2018, 19, 838-846.	0.5	36
60	Nuclear Cardiology. European Heart Journal, 2018, 39, 913-913.	1.0	0
61	Head-to-head comparison of adaptive statistical and model-based iterative reconstruction algorithms for submillisievert coronary CT angiography. European Heart Journal Cardiovascular Imaging, 2018, 19, 193-198.	0.5	24
62	Age- and sex-dependent changes in sympathetic activity of the left ventricular apex assessed by 18F-DOPA PET imaging. PLoS ONE, 2018, 13, e0202302.	1.1	29
63	Sex differences in the long-term prognostic value of 13N-ammonia myocardial perfusion positron emission tomography. European Journal of Nuclear Medicine and Molecular Imaging, 2018, 45, 1964-1974.	3.3	21
64	Hybrid SPECT Perfusion Imaging and Coronary CT Angiography: Long-term Prognostic Value for Cardiovascular Outcomes. Radiology, 2018, 288, 694-702.	3.6	35
65	Basic principles and technological state of the art: hybrid imaging. , 2018, , .		Ο
66	Basic principles and technological state of the art: hybrid imaging. , 2018, , 579-582.		0
67	Hybrid CCTA/SPECT myocardial perfusion imaging findings in patients with anomalous origin of coronary arteries from the opposite sinus and suspected concomitant coronary artery disease. Journal of Nuclear Cardiology, 2017, 24, 226-234.	1.4	34
68	Real-time respiratory triggered SPECT myocardial perfusion imaging using CZT technology: impact of respiratory phase matching between SPECT and low-dose CT for attenuation correction. European Heart Journal Cardiovascular Imaging, 2017, 18, 31-38.	0.5	12
69	Attenuation correction in stress-only myocardial perfusion imaging. Journal of Nuclear Cardiology, 2017, 24, 402-404.	1.4	5
70	A low-dose and an ultra-low-dose contrast agent protocol for coronary CT angiography in a clinical setting: quantitative and qualitative comparison to a standard dose protocol. British Journal of Radiology, 2017, 90, 20160933.	1.0	12
71	Long-term prognostic performance of low-dose coronary computed tomography angiography with prospective electrocardiogram triggering. European Radiology, 2017, 27, 4650-4660.	2.3	21
72	Long-term outcome prediction by functional parameters derived from coronary computed tomography angiography. International Journal of Cardiology, 2017, 243, 533-537.	0.8	12

#	Article	IF	CITATIONS
73	Third-degree atrioventricular block: tip of the iceberg of a systemic disease. European Heart Journal, 2017, 38, 1349-1349.	1.0	3
74	Outcome in middle-aged individuals with anomalous origin of the coronary artery from the opposite sinus: a matched cohort study. European Heart Journal, 2017, 38, 2009-2016.	1.0	41
75	Fused cardiac hybrid imaging with coronary computed tomography angiography and positron emission tomography in patients with complex coronary artery anomalies. Congenital Heart Disease, 2017, 12, 49-57.	0.0	21
76	Diagnostic accuracy of coronary opacification derived from coronary computed tomography angiography to detect ischemia: first validation versus single-photon emission computed tomography. EJNMMI Research, 2017, 7, 92.	1.1	5
77	Absolute Myocardial Blood Flow and Flow Reserve Assessed by Gated SPECT with Cadmium–Zinc–Telluride Detectors Using ^{99m} Tc-Tetrofosmin: Head-to-Head Comparison with ¹³ N-Ammonia PET. Journal of Nuclear Medicine, 2016, 57, 1887-1892.	2.8	110
78	Adaptive Statistical Iterative Reconstruction-V. Journal of Computer Assisted Tomography, 2016, 40, 958-963.	0.5	39
79	Minimized Radiation and Contrast Agent Exposure for Coronary Computed Tomography Angiography: First Clinical Experience on a Latest Generation 256-slice Scanner. Academic Radiology, 2016, 23, 1008-1014.	1.3	48
80	Left Main Artery Thrombus Complicating Heart Transplantation in a Patient With Heparin-Induced Thrombocytopenia. Journal of Cardiothoracic and Vascular Anesthesia, 2016, 30, 1334-1336.	0.6	5
81	Quantification of epicardial and intrathoracic fat volume does not provide an added prognostic value as an adjunct to coronary artery calcium score and myocardial perfusion single-photon emission computed tomography. European Heart Journal Cardiovascular Imaging, 2016, 17, 885-891.	0.5	11
82	Prevalence and characteristics of coronary artery anomalies detected by coronary computed tomography angiography in 5 634 consecutive patients in a single centre in Switzerland. Swiss Medical Weekly, 2016, 146, w14294.	0.8	32
83	MR-based attenuation correction for cardiac FDG PET on a hybrid PET/MRI scanner: comparison with standard CT attenuation correction. European Journal of Nuclear Medicine and Molecular Imaging, 2015, 42, 1574-1580.	3.3	48
84	Three-Dimensional Fusion Display of CT Coronary Angiography and Myocardial Perfusion. , 2015, , 195-206.		0
85	Recovery mismatch between myocardial blood flow and cardiac workload after physical exercise: a positron emission tomography study. European Heart Journal Cardiovascular Imaging, 2014, 15, 1386-1390.	0.5	Ο
86	Orthostatic Hypotension Appears to be Common Among Lung Transplant Recipients. Chest, 2014, 145, 633A.	0.4	2
87	Myocardial perfusion imaging with 13N-Ammonia PET is a strong predictor for outcome. International Journal of Cardiology, 2013, 167, 1023-1026.	0.8	33
88	Nonmelanoma Skin Cancer in Organ Transplant Recipients: Increase Without Delay After Transplant and Subsequent Acceleration. JAMA Dermatology, 2013, 149, 618.	2.0	12
89	Diagnostic Value of ¹³ N-Ammonia Myocardial Perfusion PET: Added Value of Myocardial Flow Reserve. Journal of Nuclear Medicine, 2012, 53, 1230-1234.	2.8	182
90	Coronary Calcium Score as an Adjunct to Nuclear Myocardial Perfusion Imaging for Risk Stratification Before Noncardiac Surgery. Journal of Nuclear Medicine, 2012, 53, 1081-1086.	2.8	25

#	Article	lF	CITATIONS
91	Cadmium-Zinc-Telluride Myocardial Perfusion Imaging in Obese Patients. Journal of Nuclear Medicine, 2012, 53, 1401-1406.	2.8	57
92	Prognostic value of coronary vessel dominance in relation to significant coronary artery disease determined with non-invasive computed tomography coronary angiography. European Heart Journal, 2012, 33, 1367-1377.	1.0	58
93	Psychometric characteristics of the German adaptation of the Traumatic Experiences Checklist (TEC) Psychological Trauma: Theory, Research, Practice, and Policy, 2012, 4, 338-346.	1.4	9
94	Age- and gender-specific differences in the prognostic value of CT coronary angiography. Heart, 2012, 98, 232-237.	1.2	22
95	Image quality and radiation dose comparison of prospectively triggered low-dose CCTA: 128-slice dual-source high-pitch spiral versus 64-slice single-source sequential acquisition. International Journal of Cardiovascular Imaging, 2012, 28, 1217-1225.	0.7	46
96	Downstream resource utilization following hybrid cardiac imaging with an integrated cadmium-zinc-telluride/64-slice CT device. European Journal of Nuclear Medicine and Molecular Imaging, 2012, 39, 430-436.	3.3	27
97	Low-Dose Computed Tomography Coronary Angiography With Prospective Electrocardiogram Triggering. Journal of the American College of Cardiology, 2011, 57, 332-336.	1.2	84
98	Semiconductor Detectors Allow Low-Dose–Low-Dose 1-Day SPECT Myocardial Perfusion Imaging. Journal of Nuclear Medicine, 2011, 52, 1204-1209.	2.8	56
99	Rapid cardiac hybrid imaging with minimized radiation dose for accurate non-invasive assessment of ischemic coronary artery disease. International Journal of Cardiology, 2011, 153, 10-13.	0.8	16
100	Very high coronary calcium score unmasks obstructive coronary artery disease in patients with normal SPECT MPI. Heart, 2011, 97, 998-1003.	1.2	67
101	Impact of CT attenuation correction on the viability pattern assessed by 99mTc-tetrofosmin SPECT/18F-FDG PET. International Journal of Cardiovascular Imaging, 2011, 27, 913-921.	0.7	10
102	Nuclear myocardial perfusion imaging with a novel cadmium-zinc-telluride detector SPECT/CT device: first validation versus invasive coronary angiography. European Journal of Nuclear Medicine and Molecular Imaging, 2011, 38, 2025-2030.	3.3	78
103	Left ventricular dyssynchrony assessment by phase analysis from gated PET-FDG scans. Journal of Nuclear Cardiology, 2011, 18, 920-925.	1.4	29
104	Main pulmonary artery diameter from attenuation correction CT scans in cardiac SPECT accurately predicts pulmonary hypertension. Journal of Nuclear Cardiology, 2011, 18, 634-641.	1.4	21
105	Linear Response Equilibrium versus echo-planar encoding for fast high-spatial resolution 3D chemical shift imaging. Journal of Magnetic Resonance, 2011, 211, 80-88.	1.2	0
106	Prognostic performance of low-dose coronary CT angiography with prospective ECG triggering. Heart, 2011, 97, 1385-1390.	1.2	15
107	Influence of smoking on the prognostic value of cardiovascular computed tomography coronary angiography. European Heart Journal, 2011, 32, 365-370.	1.0	13
108	Prognostic value of cardiac hybrid imaging integrating single-photon emission computed tomography with coronary computed tomography angiography. European Heart Journal, 2011, 32, 1465-1471.	1.0	127

#	Article	IF	CITATIONS
109	Inter-scan variability of coronary artery calcium scoring assessed on 64-multidetector computed tomography vs. dual-source computed tomography: a head-to-head comparison. European Heart Journal, 2011, 32, 1865-1874.	1.0	71
110	Impact of cardiac hybrid single-photon emission computed tomography/computed tomography imaging on choice of treatment strategy in coronary artery disease. European Heart Journal, 2011, 32, 2824-2829.	1.0	64
111	Improved Outcome Prediction by SPECT Myocardial Perfusion Imaging After CT Attenuation Correction. Journal of Nuclear Medicine, 2011, 52, 196-200.	2.8	73
112	Long-term prognostic value of left ventricular dyssynchrony assessment by phase analysis from myocardial perfusion imaging. Heart, 2011, 97, 33-37.	1.2	68
113	Incidental Detection of a Pulmonary Adenocarcinoma on Low-Dose Computed Tomography Used for Attenuation Correction in Myocardial Perfusion Imaging With SPECT. Clinical Nuclear Medicine, 2010, 35, 751-752.	0.7	6
114	Coronary calcium score scans for attenuation correction of quantitative PET/CT 13N-ammonia myocardial perfusion imaging. European Journal of Nuclear Medicine and Molecular Imaging, 2010, 37, 517-521.	3.3	27
115	Non-invasive assessment of coronary artery disease with CT coronary angiography and SPECT: a novel dose-saving fast-track algorithm. European Journal of Nuclear Medicine and Molecular Imaging, 2010, 37, 522-527.	3.3	33
116	New reconstruction algorithm allows shortened acquisition time for myocardial perfusion SPECT. European Journal of Nuclear Medicine and Molecular Imaging, 2010, 37, 750-757.	3.3	48
117	Ultrafast nuclear myocardial perfusion imaging on a new gamma camera with semiconductor detector technique: first clinical validation. European Journal of Nuclear Medicine and Molecular Imaging, 2010, 37, 773-778.	3.3	165
118	Real-time breath-hold triggering of myocardial perfusion imaging with a novel cadmium-zinc-telluride detector gamma camera. European Journal of Nuclear Medicine and Molecular Imaging, 2010, 37, 1903-1908.	3.3	38
119	Ultrafast assessment of left ventricular dyssynchrony from nuclear myocardial perfusion imaging on a new high-speed gamma camera. European Journal of Nuclear Medicine and Molecular Imaging, 2010, 37, 2086-2092.	3.3	39
120	Myocardial perfusion imaging with real-time respiratory triggering: Impact of inspiration breath-hold on left ventricular functional parameters. Journal of Nuclear Cardiology, 2010, 17, 848-852.	1.4	12
121	Validation of a new contrast material protocol adapted to body surface area for optimized low-dose CT coronary angiography with prospective ECG-triggering. International Journal of Cardiovascular Imaging, 2010, 26, 591-597.	0.7	44
122	Nuclear Myocardial Perfusion Imaging with a Cadmium-Zinc-Telluride Detector Technique: Optimized Protocol for Scan Time Reduction. Journal of Nuclear Medicine, 2010, 51, 46-51.	2.8	195
123	Validation of CT Attenuation Correction for High-Speed Myocardial Perfusion Imaging Using a Novel Cadmium-Zinc-Telluride Detector Technique. Journal of Nuclear Medicine, 2010, 51, 1539-1544.	2.8	59
124	The Validity and Reliability of the German Version of the Somatoform Dissociation Questionnaire (SDQ-20). Journal of Trauma and Dissociation, 2010, 11, 337-357.	1.0	38
125	Cardiac hybrid imaging with high-speed single-photon emission computed tomography/CT camera to detect ischaemia and coronary artery obstruction. Heart, 2010, 96, 2050-2050.	1.2	10
126	Usefulness of Additional Coronary Calcium Scoring in Low-dose CT Coronary Angiography with Prospective ECG-Triggering. Academic Radiology, 2010, 17, 201-206.	1.3	27

#	Article	IF	CITATIONS
127	Prevalence of noncardiac findings on low dose 64-slice computed tomography used for attenuation correction in myocardial perfusion imaging with SPECT. International Journal of Cardiovascular Imaging, 2009, 25, 859-865.	0.7	23
128	Incremental prognostic value of multi-slice computed tomography coronary angiography over coronary artery calcium scoring in patients with suspected coronary artery disease. European Heart Journal, 2009, 30, 2622-2629.	1.0	147